Zero-field quantum critical point in $Ce_{0.91}Yb_{0.09}CoIn_5$

Y. P. Singh,[1,*] R. B. Adhikari,[1] D. J. Haney,[1] B. D. White,[2,3,4] M. B. Maple,[2,3,4] M. Dzero,[1] and C. C. Almasan[1]

[1]*Department of Physics, Kent State University, Kent, Ohio 44242, USA*

[2]*Center for Advanced Nanoscience, University of California, San Diego, La Jolla, California 92093, USA*

[3]*Materials Science and Engineering Program, University of California, San Diego, La Jolla, California 92093, USA*

[4]*Department of Physics, University of California at San Diego, La Jolla, California 92903, USA*

(Received 20 September 2017; revised manuscript received 9 April 2018; published 24 May 2018)

We present results of specific heat, electrical resistance, and magnetoresistivity measurements on single crystals of the heavy-fermion superconducting alloy $Ce_{0.91}Yb_{0.09}CoIn_5$. Non-Fermi-liquid to Fermi-liquid crossovers are clearly observed in the temperature dependence of the Sommerfeld coefficient γ and resistivity data. Furthermore, we show that the Yb-doped sample with $x = 0.09$ exhibits universality due to an underlying quantum phase transition without an applied magnetic field by utilizing the scaling analysis of γ. Fitting of the heat capacity and resistivity data based on existing theoretical models indicates that the zero-field quantum critical point is of antiferromagnetic origin. Finally, we found that at zero magnetic field the system undergoes a third-order phase transition at the temperature $T_{c3} \approx 7$ K.

DOI: 10.1103/PhysRevB.97.184514

I. INTRODUCTION

The study of quantum critical behavior of modern materials continues to be a central topic in condensed-matter physics since quantum phase transitions (QPTs) at a quantum critical point (QCP) can drive a system away from its normal metallic behavior, resulting in distinctly different physical properties in the vicinity of QCP [1,2]. In unconventional superconductors, such as heavy-fermion (HF) materials, cuprates, and pnictides, the presence of competing interactions, due to the proximity of antiferromagnetism and superconductivity, can give rise to zero-point critical fluctuations and to a QPT from a magnetically ordered to a disordered phase. This raises the possibility that the unconventional superconducting pairing in these systems is mediated by antiferromagnetic (AFM) spin fluctuations. In addition, many of these systems exhibit deviation from their Fermi-liquid properties in the presence of a QCP. Hence these materials offer great potential to study and understand the nature of unconventional superconductivity (SC).

$Ce_{1-x}Yb_xCoIn_5$ is an intriguing HF system which has attracted much attention because many of the properties observed in this material do not conform to those of similar HF superconductors [3–5]. The parent compound $CeCoIn_5$ is an example of a metal in which the system's proximity to a QPT between the paramagnetic and AFM states is controlled by thermodynamic variables such as magnetic field (H) or pressure, with the antiferromagnetic ground state superseded by superconductivity [6–9]. Substitution of Ce by Yb results in a gradual suppression of the magnetic-field-driven QCP (H_{QCP}) to zero in the vicinity of the Yb doping level $x = 0.07$ [10], suggesting that there exists a critical concentration x_c at which the low-T properties of $Ce_{1-x_c}Yb_{x_c}CoIn_5$ are of a quantum critical metal. In addition, recent reports reveal a significant modification of the Fermi surface of $Ce_{1-x}Yb_xCoIn_5$ with Yb substitution [11] and its doping-dependent change from a nodal to a nodeless gap [12]. All these studies have led the way to proposals of new, exciting possibilities such as a composite pairing mechanism and topological superconductivity [13] and two different Fermi surfaces contributing to charge transport [14]. However, an extremely important question pertains to the role played by quantum critical fluctuations in determining the symmetry of the superconducting gap and system's thermodynamic and transport properties.

Here, we present results of thermodynamic and transport studies of the superconducting alloy $Ce_{0.91}Yb_{0.09}CoIn_5$ tailored to address the above question in the $Ce_{1-x}Yb_xCoIn_5$ heavy-fermion family. Our study reveals a clear correlation between critical spin fluctuations and unconventional superconductivity. Specifically, the presence of a crossover from a Fermi-liquid (FL) to a non-Fermi-liquid (NFL) regime along with the scaling analysis of the Sommerfeld coefficient demonstrate that the normal state of $Ce_{0.91}Yb_{0.09}CoIn_5$ is quantum critical. Furthermore, our analysis reveals that the underlying quantum phase transition is of magnetic nature, separating antiferromagnetic and paramagnetic phases. These present results along with the results from Ref. [12] indicate that the nodal gap structure and unconventional superconductivity in $Ce_{1-x}Yb_xCoIn_5$ for Yb doping x smaller than the critical value x_c is due to the presence of AFM critical spin fluctuations near a QCP, while for $x > x_c$ the critical fluctuations are fully suppressed and this system displays conventional SC. Our present results also show that quantum criticality emerges for Yb concentrations for which Yb is in a magnetic valence configuration that seems to play a crucial role in preserving the long-range order of the diluted Ce lattice and stabilizing the unconventional superconducting state in this fascinating material. Finally, we also found that at $H = 0$ the system

*Present address: Department of Mechanical Engineering, The University of Akron, Akron, Ohio 44325, USA.

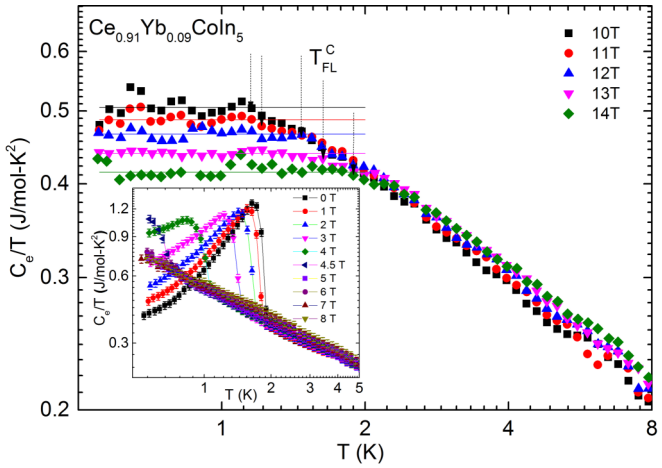

FIG. 1. Log-log plot of Sommerfeld coefficient $\gamma \equiv C_e(T)/T$ (C_e is the electronic specific heat) vs temperature T of $Ce_{0.91}Yb_{0.09}CoIn_5$ measured with applied magnetic field $H \| c$ axis over the temperature range $0.50 \leqslant T \leqslant 10$ K and $10 \leqslant H \leqslant 14$ T. The horizontal lines are fits of the data. The temperature $T_{\rm FL}^C$, marked by the arrows, is the crossover temperature from the Fermi-liquid (T-independent γ) to the non-Fermi-liquid (γ has power-law-in-T dependence) regime. Inset: Log-log plot of C_e/T vs T, measured in $0 \leqslant H \leqslant 8$ T.

undergoes a third-order phase transition at the temperature $T_{c3} \approx 7$ K.

II. EXPERIMENTAL DETAILS

Single crystals of $Ce_{0.91}Yb_{0.09}CoIn_5$ were grown using an indium self-flux method [15]. They were etched in concentrated HCl to remove the indium left on the surface during the growth process and were then rinsed thoroughly in ethanol. The crystal structure and unit cell volume were determined from x-ray powder diffraction measurements, while the actual Yb composition x for the samples studied here was determined according to the method developed by Jang *et al.* [16]. We note that we will refer to nominal Yb concentration x_n when we mention previous results that report only this value. The single crystals studied have a typical size of $2.1 \times 1.0 \times 0.16$ mm^3, with the c axis along the shortest dimension of the crystals.

Heat capacity measurements were performed under magnetic fields up to 14 T, applied parallel to the c axis ($H \| c$) of the crystals and for temperatures as low as 0.50 K. The data was obtained in a Quantum Designs Physical Property Measurement System using semi-adiabatic calorimetry and utilizing the heat pulse technique.

Four leads were attached to the single crystals, with the current $I \| a$ axis, using a silver-based conductive epoxy. We performed in-plane electrical resistance (R) measurements between 0.50 and 300 K and transverse magnetoresistivity (MR) $\triangle\rho \equiv [\rho(H) - \rho(H=0)]/\rho(H=0)$ measurements as a function of temperature between 2 and 300 K and transverse magnetic field ($H \perp I$) up to 14 T.

III. RESULTS AND DISCUSSION

In Fig. 1 we show the temperature dependence of the Sommerfeld coefficient $\gamma \equiv C_e(T)/T$ of $Ce_{0.91}Yb_{0.09}CoIn_5$ measured in $10 \leqslant H \leqslant 14$ T and at low temperatures ($0.5 \leqslant T \leqslant 8$ K). We obtained the electronic specific heat C_e after subtracting a large Schottky anomaly tail due to the quadrupolar and magnetic spin splitting of Co and In nuclei [17]. All the data shown in this figure represent normal-state results since the superconducting transition temperature is gradually suppressed with increasing magnetic field and approaches 0.5 K (the lowest temperature of the heat capacity measurements performed here) for a field of 4.5 T (see inset to Fig. 1). Notice that all the data shown in the main panel of Fig. 1 display a crossover between a constant γ at low temperatures and a power-law T-dependent γ at higher T, with $\gamma \approx 0.52/T^{0.48}$, supported by the data analysis shown in the left inset of Fig. 3. The former behavior is typical of the FL state, while the latter reflects a non-Fermi-liquid state. We define as $T_{\rm FL}^{\rm C}$ (arrows in the main panel of Fig. 1) the temperature at which $\gamma(T)$ deviates from the horizontal line, i.e., where it changes from the FL region to the NFL (power-law-in-T dependence) region.

The presence of critical fluctuations as well as the FL to NFL crossover observed in both heat capacity and resistivity (see the Supplemental Material for the analysis of resistivity and heat capacity data [18]) suggest the presence of a second-order QPT at a QCP. Quantum phase transitions are different from conventional thermodynamic transitions in that the correlations of the incipient order parameter fluctuate on a characteristic energy scale $E_0 \gg k_B T_c$, where T_c is the critical temperature, which in our system is vanishingly small. This energy scale E_0 becomes also vanishingly small as the host system is tuned to QCP [2] by varying thermodynamic variables such as magnetic field and pressure or by changing the chemical composition, and temperature remains the only energy scale which controls the physics at low temperatures. As a result, the system's thermodynamic properties are dominated by the continuum of thermally excited quantum critical fluctuations at low enough temperatures, $k_B T \ll E_0$. Consequently, the specific heat and magnetic susceptibility exhibit anomalous power-law temperature dependences, which can be accounted for by exponents whose values are determined by the nature of the order parameter fluctuations and the relative strength of the interactions between the quantum critical fluctuations. Perhaps the most recent example of this has been provided by Wölfle and Abrahams, who have argued that an interplay between the non-Gaussian quantum critical fluctuations and itinerant fermionic quasiparticles leads to the anomalous temperature dependence of the Sommerfeld coefficient, $\gamma \propto 1/T^{0.25}$, in the quantum critical metal $YbRu_2Si_2$ [19,20].

In order to verify that the concentration $x_c = 0.09$ corresponds to a critical value at which $E_0(x = x_c) \to 0$, we generated the H-T phase diagram shown in Fig. 2. The FL to NFL crossovers are extracted from heat capacity and resistance measurements as $T_{\rm FL}^{\rm C}(H)$ (black squares) and $T_{\rm FL}^{R}(H)$ (red circles), respectively, as discussed above and in the Supplemental Material [18]. The $T_c(H)$ boundary separating metallic and superconducting phases is obtained from the resistance and heat capacity measurements. Notice that the FL to NFL crossovers obtained from the two measurements are in excellent agreement. Linear extrapolations of these crossovers to zero temperature, under the superconducting dome, give the value of $H_{\rm QCP}$. Figure 2 clearly shows that these linear

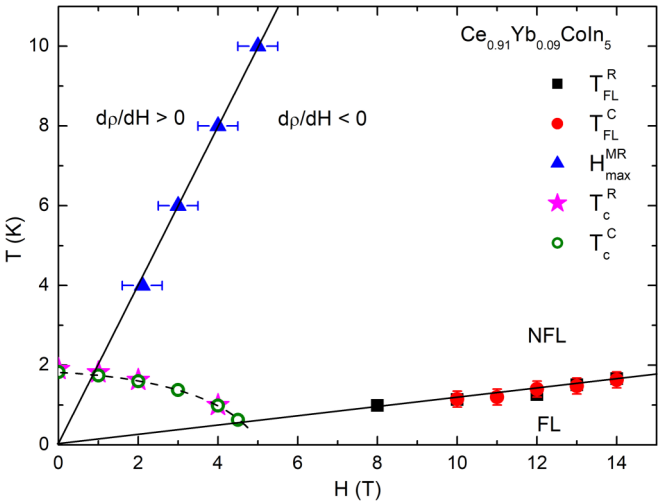

FIG. 2. Temperature–magnetic-field (T-H) phase diagram of $Ce_{0.91}Yb_{0.09}CoIn_5$ with $H \| c$ axis. The area under the dotted line represents the superconducting region. The straight lines are linear fits of the data extrapolated to zero temperature. $H_{\max}^{MR}$ is the peak in the H dependence of magnetoresistivity, MR (see Supplemental Material for details [18]). T_{FL}^{R} and T_{FL}^{C} are the temperatures at which the data cross from a Fermi-liquid to a non-Fermi-liquid regime, measured by electrical resistance and heat capacity, respectively. Likewise, T_c^R and T_c^C is the superconducting transition temperature measured by electrical resistance and heat capacity, respectively.

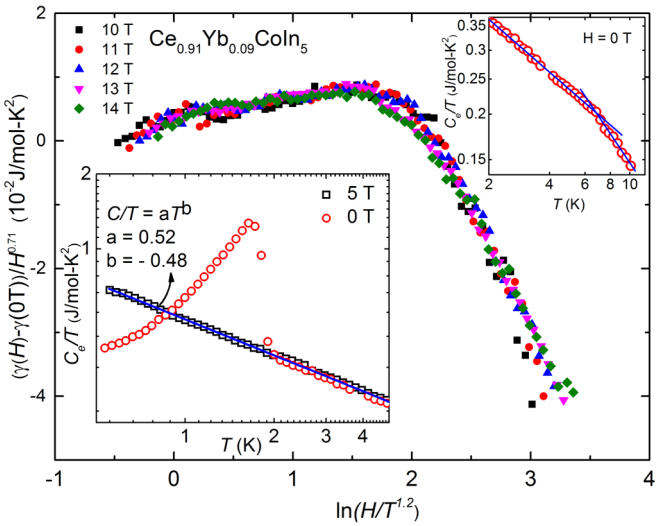

FIG. 3. Scaling of γ according to the function $\gamma(H) - \gamma(H_{\rm QCP}) \sim (H - H_{\rm QCP})^{0.71} f((H - H_{\rm QCP})/T^{1.2})$ with $H_{QCP} = 0T$. We obtained the best scaling shown on the main panel with a power-law dependence of $\gamma(0)$ at temperatures $T \leqslant 5$ K. Bottom inset: Log-Log plot of 0 and 5 T data and their normal state fit with $C_e/T = 0.52/T^{0.48}$. Top inset: Log-log plot of C_e/T vs T data measured in $H = 0$ to show the third-order phase transition.

extrapolations give $H_{\rm QCP} = 0$, indicating that 9% Yb is the critical doping, i.e., $x_c = 0.09$ for the $Ce_{1-x}Yb_xCoIn_5$ system. Additional evidence comes from our analysis of magnetoresistivity (MR) data measured in different applied magnetic fields (see the Supplemental Material [18]). Specifically, a linear extrapolation of the peak in MR at $H_{\max}^{MR}$ (blue triangles in Fig. 2) to zero temperature again results in $H_{\rm QCP} = 0$ T. It is also worth mentioning here that the $Ce_{1-x}Yb_xCoIn_5$ system exhibits a crossover at $x = 0.09$ from a Kondo lattice ($x < 0.09$) to a single-ion Kondo regime ($x > 0.09$) [21]. In other words, the Ce ions in the latter case do not form a lattice, hence, the possibility of a magnetically ordered phase can be ruled out for Yb doping $x > 0.09$.

Finally, in order to confirm that the anomalous temperature dependence of the Sommerfeld coefficient $\gamma(H,T)$ is governed by quantum critical fluctuations, we show that $\gamma(H,T)$ is governed by the critical free energy density $f_{\rm cr} = a_0 r^{\nu(d+z)} f_0(T/r^{\nu z}) = a_0 T^{(d+z)/z} \tilde{f}_0(r/T^{1/\nu z})$, where a_0 is a constant, f_0 and $\tilde{f}_0$ are scaling functions, $r \propto (H - H_{\rm QCP})$, d is the dimensionality of the system, z is the dynamical critical exponent, and ν is the correlation length exponent. By comparing the Sommerfeld coefficient $\gamma_{\rm cr} = (\partial^2 f_{\rm cr}/\partial T^2)$ with the experimentally measured one at $H = 0$ (inset to Fig. 3), we find $d = 0.52z$. Furthermore, at finite magnetic fields, we were able to scale the data by choosing $\nu(d - z) = 0.71$ and $1/\nu z = 1.2$ (see Fig. 3). We note that the $1/\sqrt{T}$ divergence of the Sommerfeld coefficient is fully consistent with the universal restriction $1/\nu z < 3/2$ [22]. Lastly, we point out that the critical exponent $\alpha = 1 + d/z$ for $\gamma(T, H = 0) \sim T^{-\alpha}$ is governed by the universality class of ordinary percolation.

The result of the scaling is shown in Fig. 3. We obtained a very good scaling with the normal-state zero-field $\gamma(T,0) = 0.52/T^b$, with $b = 0.48$. The scaling of γ covers both the FL range (present at low T) and the NFL range (present at higher T), with a small amount of scatter near the FL to NFL crossover temperature. We attribute this to the lack of a sharp crossover for magnetic fields of 13 and 14 T, as seen in Fig. 1. A peculiar feature of our scaling plot is the existence of a hump for $\log(H/T^{1.2}) \in [1.5,2]$ followed by a decrease at higher temperatures. This is a result of the power-law divergence of the Sommerfeld coefficient at the quantum critical field, which in this case is $H_{QCP} = 0$. This feature should be clearly absent if the Sommerfeld coefficient has a logarithmic divergence with temperature, as is the case for $CeCoIn_5$ (see Fig. 1(b) of Ref. [6]).

We note that although both $Ce_{0.91}Yb_{0.09}CoIn_5$ and $YbRu_2Si_2$ have antiferromagnetic QCPs, the value of the exponent $b = 0.48$ in $Ce_{0.91}Yb_{0.09}CoIn_5$ exceeds the one for $YbRu_2Si_2$ ($b = 0.25$) [23]. This implies perhaps a different character of the interplay between the critical fluctuations and fermionic degrees of freedom.

The challenge in obtaining the scaling shown in Fig. 3 was to determine the normal-state zero-field $\gamma(T,0)$ at low temperatures since this sample becomes superconducting for temperatures below ~2 K. We overcame this problem by determining the T dependence of the metallic $\gamma(T, 5\ \text{T})$ down to 0.5 K. We obtained a power-law T dependence of the form $\gamma(T, 5\ \text{T}) = 0.52/T^{0.48}$ by fitting these data. (see the blue line in the inset to Fig. 3). These data are in the NFL regime over this temperature range, with a crossover to the FL regime at $T \approx 0.4$ K (see Fig. 2). This procedure is supported by the fact that the normal-state $\gamma(T,H)$, exposed at low temperature by the application of a magnetic field, follows

a power-law behavior, clearly visible for fields up to 8 T and temperatures as low as 0.5 K, as shown in the inset to Fig. 1. In addition, we confirmed that the normal-state $\gamma(T,0)$ of $Ce_{0.91}Yb_{0.09}CoIn_5$ diverges as $\gamma(T,0) \approx 0.52/T^{0.48}$, not as $-\log T$, as $T \to 0$ by showing that the normal-state and superconducting entropies are equal at T_c (see the discussion and figure in the Supplemental Material [18]).

This scaling analysis, together with the phase diagram of Fig. 2, generated based on the FL to NFL crossover in $\gamma(T)$ and $R(T)$, serve as evidence that there is a second-order QPT with $H_{QCP} = 0$ for the $x_c = 0.09$ $Ce_{1-x}Yb_xCoIn_5$ alloy. Hence, $Ce_{0.91}Yb_{0.09}CoIn_5$ is, indeed, a zero-field quantum critical metal at ambient pressure. We have shown previously that H_{QCP} of the $Ce_{1-x}Yb_xCoIn_5$ system is suppressed from about 4.1 T for $CeCoIn_5$ to close to zero for $x = 0.07$ [10]. This is consistent with the present finding that the higher doping of $x = 0.09$ ($x_n = 0.25$) is the critical doping. In addition, changes in the Fermi surface topology of $Ce_{1-x}Yb_xCoIn_5$ have been revealed by de Haas–van Alphen studies, which found the disappearance of the intermediately heavy α sheet for $0.1 \leqslant x_n \leqslant 0.2$ [11]. This result correlates with a study of the electronic structure of $Ce_{1-x}Yb_xCoIn_5$, which has shown that the Yb valence for $x_n \leqslant 0.2$ increases rapidly from $Yb^{2.3+}$ toward Yb^{3+} with decreasing x [24]. Also, recent penetration depth measurements on $Ce_{1-x}Yb_xCoIn_5$ have reported that the superconducting gap changes its character around $x \approx 0.037$ ($x_n = 0.2$) from nodal to nodeless with increasing Yb doping [12]. Hence, all these findings indicate that the following features are present at $x_c \approx 0.09$ ($x_n = 0.25$): Fermi surface reconstruction, Yb valence transition from Yb^{3+} to $Yb^{2.3+}$ (the Ce valence is 3+ for all x values), transition from nodal to nodeless superconductivity, and suppression of H_{QCP} towards 0 T. We note that $T_c(x)$ decreases linearly with x [10], without any features near $x_c = 0.09$.

Based on these results, one is tempted to speculate that the nodal gap structure and unconventional superconductivity in $Ce_{1-x}Yb_xCoIn_5$ can be attributed to the presence of AFM critical spin fluctuations near a QCP for $x < x_c = 0.09$. We note that in many cases critical spin fluctuations lead to the formation of a nodal gap [25]. With increasing Yb doping beyond x_c, this system displays conventional SC in which the emergence of SC and onset of many-body coherence in the Kondo lattice have the same physical origin: hybridization between conduction and localized Ce $4f$-electron states [10]. We note that the presence of Yb as the substitution for Ce provides a unique scenario in which quantum criticality is observed for Yb doping for which Yb exhibits a magnetic valence. In this sense, the magnetic valence of Yb might have a role in preserving the long-range order of the diluted Ce lattice, and, thereby, facilitating the magnetic order and the development of a quantum phase transition in this system. At the same time, the robustness of unconventional superconductivity with respect to disorder points towards the multiband nature of superconductivity: intraband disorder scattering is dominant, while pairing involves several bands and therefore remains largely immune to disorder.

Our analysis of the specific heat data for $H = 0$ also reveals a discontinuous change in slope of C/T as a function of T at $T_{c3} \approx 7$ K (right inset of Fig. 3). This means that the third derivative of the free energy with respect to temperature is discontinuous and, therefore, the system undergoes a *third-order phase transition* at $T = T_{c3}$. We leave for future studies the possible origin of this transition and whether it is governed by the underlying quantum critical fluctuations.

IV. SUMMARY

To conclude, we performed specific heat, electrical resistance, and magnetoresistivity measurements on single crystals of the heavy-fermion superconducting alloy $Ce_{0.91}Yb_{0.09}CoIn_5$ and showed that this material is quantum critical, i.e., it has an antiferromagnetic QCP in zero magnetic field and at ambient pressure. Hence, the physical properties of this material in the normal state at low temperatures are controlled by the presence of this QCP. The existence of this QCP is confirmed by the scaling analysis of the specific heat data. The AFM nature of this QCP is suggested by the excellent fits of both heat capacity and resistance data measured in different magnetic fields with the spin fluctuation theory [26]. Our findings, along with other recent reports on this system, suggest that the origin of the superconducting pairing is different in samples with low and high Yb doping: The presence of AFM fluctuations is most likely the reason for the nodal gap at lower doping, while the fact that $x_c = 0.09$ for $Ce_{1-x}Yb_xCoIn_5$, hence there are no AFM fluctuations for $x \geqslant 0.09$, implies that a conventional pairing mechanism gives the nodeless characteristics of the superconducting gap.

ACKNOWLEDGMENTS

This work was supported by the National Science Foundation Grants No. DMR-1505826 and No. DMR-1506547 at KSU and by the US Department of Energy, Office of Basic Energy Sciences, Division of Materials Sciences and Engineering, under Grants No. DE-SC0016481 at KSU and No. DE-FG02-04ER46105 at UCSD. M.D. also acknowledges the hospitality of the Kirchhoff Institute of Physics (University of Heidelberg), where part of this work was completed.

Y.P.S. and R.B.A. contributed equally to this work.

[1] P. Coleman and A. J. Schofield, Nature (London) **433**, 226 (2005).

[2] H. V. Löhneysen, A. Rosch, M. Vojta, and P. Wölfle, Rev. Mod. Phys. **79**, 1015 (2007).

[3] L. Shu, R. E. Baumbach, M. Janoschek, E. Gonzales, K. Huang, T. A. Sayles, J. Paglione, J. O'Brien, J. J. Hamlin, D. A. Zocco *et al.*, Phys. Rev. Lett. **106**, 156403 (2011).

[4] B. D. White, J. J. Hamlin, K. Huang, L. Shu, I. K. Lum, R. E. Baumbach, M. Janoschek, and M. B. Maple, Phys. Rev. B **86**, 100502 (2012).

[5] Y. Xu, J. K. Dong, I. K. Lum, J. Zhang, X. C. Hong, L. P. He, K. F. Wang, Y. C. Ma, C. Petrovic, M. B. Maple *et al.*, Phys. Rev. B **93**, 064502 (2016).

[6] A. Bianchi, R. Movshovich, I. Vekhter, P. G. Pagliuso, and J. L. Sarrao, Phys. Rev. Lett. **91**, 257001 (2003).
[7] J. L. Sarrao and J. D. Thompson, J. Phys. Soc. Jpn. **76**, 051013 (2007).
[8] S. Zaum, K. Grube, R. Schäfer, E. D. Bauer, J. D. Thompson, and H. v. Löhneysen, Phys. Rev. Lett. **106**, 087003 (2011).
[9] T. Hu, H. Xiao, T. A. Sayles, M. Dzero, M. B. Maple, and C. C. Almasan, Phys. Rev. Lett. **108**, 056401 (2012).
[10] T. Hu, Y. P. Singh, L. Shu, M. Janoschek, M. Dzero, M. B. Maple, and C. C. Almasan, Proc. Natl. Acad. Sci. USA **110**, 7160 (2013).
[11] A. Polyakov, O. Ignatchik, B. Bergk, K. Götze, A. D. Bianchi, S. Blackburn, B. Prévost, G. Seyfarth, M. Côté, D. Hurt *et al.*, Phys. Rev. B **85**, 245119 (2012).
[12] H. Kim, M. A. Tanatar, R. Flint, C. Petrovic, R. Hu, B. D. White, I. K. Lum, M. B. Maple, and R. Prozorov, Phys. Rev. Lett. **114**, 027003 (2015).
[13] O. Erten, R. Flint, and P. Coleman, Phys. Rev. Lett. **114**, 027002 (2015).
[14] Y. P. Singh, D. J. Haney, X. Y. Huang, B. D. White, M. B. Maple, M. Dzero, and C. C. Almasan, Phys. Rev. B **91**, 174506 (2015).
[15] E. G. Moshopoulou, Z. Fisk, J. L. Sarrao, and J. D. Thompson, J. Solid State Chem. **158**, 25 (2001).
[16] S. Jang, B. D. White, I. K. Lum, H. Kim, M. A. Tanatar, W. E. Straszheim, R. Prozorov, T. Keiber, F. Bridges, L. Shu *et al.*, Philos. Mag. **94**, 4219 (2014).
[17] R. Movshovich, M. Jaime, J. D. Thompson, C. Petrovic, Z. Fisk, P. G. Pagliuso, and J. L. Sarrao, Phys. Rev. Lett. **86**, 5152 (2001).
[18] See Supplemental Material at http://link.aps.org/supplemental/10.1103/PhysRevB.97.184514 for details of the theoretical analysis of the experimental data and the results of some of the fits of the experimental data.
[19] P. Wölfle and E. Abrahams, Phys. Rev. B **84**, 041101 (2011).
[20] P. Wölfle, J. Schmalian, and E. Abrahams, Rep. Prog. Phys. **80**, 044501 (2017).
[21] Y. P. Singh, D. J. Haney, X. Y. Huang, I. K. Lum, B. D. White, M. Dzero, M. B. Maple, and C. C. Almasan, Phys. Rev. B **89**, 115106 (2014).
[22] A. M. Tsvelik and M. Reizer, Phys. Rev. B **48**, 9887 (1993).
[23] O. Trovarelli, C. Geibel, S. Mederle, C. Langhammer, F. M. Grosche, P. Gegenwart, M. Lang, G. Sparn, and F. Steglich, Phys. Rev. Lett. **85**, 626 (2000).
[24] L. Dudy, J. D. Denlinger, L. Shu, M. Janoschek, J. W. Allen, and M. B. Maple, Phys. Rev. B **88**, 165118 (2013).
[25] K. Hashimoto, Y. Mizukami, R. Katsumata, H. Shishido, M. Yamashita, H. Ikeda, Y. Matsuda, J. A. Schlueter, J. D. Fletcher, A. Carrington *et al.*, Proc. Natl. Acad. Sci. USA **110**, 3293 (2013).
[26] T. Moriya and T. Takimoto, J. Phys. Soc. Jpn. **64**, 960 (1995).